Geomechanics and Engineering, *Vol. 14, No. 4 (2018) 355-366*
DOI: https://doi.org/10.12989/gae.2018.14.4.355

Stability of onshore pipelines in liquefied soils: Overview of computational methods

Massimina Castiglia[1a], Filippo Santucci de Magistris[*1] and Agostino Napolitano[2b]

[1]*Di.B.T Department, Structural and Geotechnical Dynamics StreGa Lab., University of Molise, via de Sanctis, 86100 Campobasso, Italy*
[2]*PRG Onshore Pipeline Specific Engineering, Saipem S.p.A., via Toniolo 1, 61032 Fano (PU), Italy*

(Received November 4, 2016, Revised August 11, 2017, Accepted August 17, 2017)

Abstract. One of the significant problems in the design of onshore pipelines in seismic areas is their stability in case of liquefaction. Several model tests and numerical analyses allow investigating the behavior of pipelines when the phenomenon of liquefaction occurs. While experimental tests contribute significantly toward understanding the liquefaction mechanism, they are costly to perform compared to numerical analyses; on the other hand, numerical analyses are difficult to execute, because of the complexity of the soil behavior in case of liquefaction.
This paper reports an overview of the existing computational methods to evaluate the stability of onshore pipelines in liquefied soils, with particular attention to the development of excess pore water pressures and the floatation of buried structures. The review includes the illustration of the mechanism of floating and the description of the available calculation methods that are classified in static and dynamic approaches. We also highlighted recent trends in numerical analyses. Moreover, for the static condition, referring to the American Petroleum Institute (API) Specification, we computed and compared the uplift safety factors in different cases that might have a relevant practical use.

Keywords: liquefaction; pipeline; flotation; computational methods

1. Introduction

Dynamic liquefaction of saturate loose sand deposits is a possible geotechnical failure effect caused by earthquakes, which can lead to large damages in natural environment (i.e., landslides or subsidence) and constructions, including buildings, infrastructures, industrial facilities and lifelines. Among them, pipeline networks constitute an important component for economic and social growth of an area. Their protection from natural hazards represents a primary challenge for engineers.

Pipelines are widely used for industrial and civil purposes for transportation of gases and liquids (natural gas, water, oils, wastewater) and are crucial infrastructures for the sustainment and development of human activities, playing an essential role in human life and in economic development. The integrity of those systems under extreme events such as earthquakes is a primary requirement, especially when they transport large amount of toxic and flammable material.

Liquefaction in the soil interacting with structures might cause permanent large displacements and consequent failure and malfunctioning of onshore pipelines induced by differential vertical settlements or horizontal lateral spread. Uplift of underground structures might also occur. As an example, Fig. 1 illustrates some cases of damages caused by liquefaction for steel buried pipelines: Fig. 1(a) refers to the Christchurch (New Zealand) earthquake in 2011 and Fig. 1(b) shows the uplift of Liquefied Petroleum Gas buried tanks during the offshore 2010 Bio-Bio (Chile) earthquake.

According to O'Rourke and Liu (1999), the dynamic behavior of the surrounding soil strongly affected the seismic response of the pipelines, especially when buried. When the soil is crossed by seismic waves, the resulting geotechnical effects related to pipeline damage are sketched in Fig. 2. They could be divided in two categories, based on experience and data collected during past earthquakes: a) Strong Ground Shaking (SGS), which causes transient deformation of soil surrounding the pipeline, without breaks or ruptures in the soil; and, b) Ground Failure (GF), due to fault displacement, liquefaction and landslides, which results in permanent deformation of soil (i.e., soil failure). The latter seismic failure mechanism appears only under specific geotechnical conditions and is site-dependent (i.e., strong motion earthquakes and presence of loose sands under groundwater level, for the liquefaction phenomenon).

We limited this research to a specific GF effect that is soil liquefaction, while other GF analyses can be found elsewhere (see, for instance, the approaches of Paolucci *et al.* 2010 and Kazem *et al.* 2013 for pipelines interacting with faults).

Pipelines, having a predominant one-dimensional development, are commonly addressed as lifelines and are often dislocated over wide areas. These structures can be installed either underground or aboveground. Usually, they

∗Corresponding author, Associate Professor
E-mail: filippo.santucci@unimol.it
[a]Ph.D. Student
E-mail: massimina.castiglia@unimol.it
[b]Onshore Pipeline Engineering Manager
E-mail: Agostino.Napolitano@saipem.com

ISSN: 2005-307X (Print), 2092-6219 (Online)

(a)

(b)

Fig. 1 Damage to industrial components induced by liquefaction, (a) steed buried pipeline (after Yamada *et al.* 2011) and (b) LPG tanks (after GEER 2010)

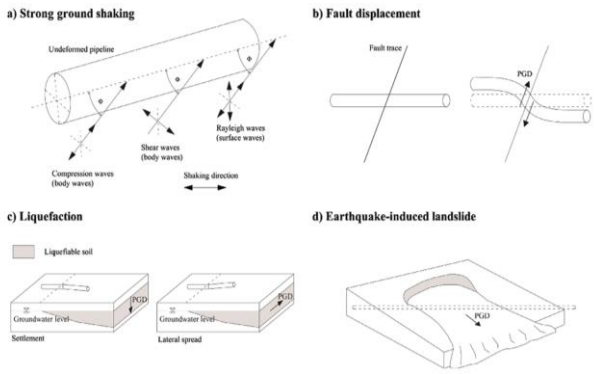

Fig. 2 Summary of strong ground shaking and ground failure interaction mechanisms (adapted after O'Rourke and Liu 1999)

are set at a burial depth of about 1-2 m. Less frequently, as in case of crossings, pipelines are buried deeper. From the observation of past earthquakes, buried pipelines appear to be vulnerable to seismic loads, even if they perform better than aboveground structures under the same conditions. The burying process is beneficial for two main reasons: the landfill protects the pipeline from external damaging events, either natural or anthropic and the lateral confinement given by the surrounding soil, which increases with depth, reduces the seismic effects. Buried pipelines tend to accommodate the soil deformation and the performances of the structures are strongly related to the geotechnical effects only.

Pipelines can be divided in two classes (e.g., Lanzano *et al.* 2015) with respect to the pre-failure deformation of the materials: ductile and brittle pipelines. Ductile pipelines show large deformations before failure and they are generally made of steel, ductile iron and high-density polyethylene; brittle pipelines, instead, fail without relevant deformations, they are made of concrete (reinforced concrete or asbestos cement) or some plastic materials, as polyvinylchloride. With respect to joints type, the pipeline can be divided in continuous and segmented. The continuous pipelines are typically characterized by strength and stiffness of the joints comparable to those observed away from the joints (e.g., welded steel, fused polyethylene, bolted joint pipe, etc.), whereas segmented pipelines show strength and stiffness of joints substantially lower than that between the joints, particularly for bell and spigot joints. The hazardous, toxic and flammable fluids must be transported only in continuous pipelines having large strength and deformation before structural breaking and consequent fluid release.

As previously stated, pipelines suffered heavy damages when loaded by seismic actions, as in the recurrent and catastrophic earthquakes of California (i.e., San Francisco, 1906; San Fernando, 1971; Northridge, 1994) and Japan (Kobe 1995). However, despite the evolution in the anti-earthquake techniques and the progress in the seismic design, relevant damages to pipelines have been still observed during recent earthquakes in Italy (L'Aquila 2009, Emilia 2012), New Zealand (Darfield 2010, Christchurch 2011), Chile (2010), Japan (Tohoku 2011), maybe because the old construction age of the damaged structures (Lanzano *et al.* 2015).

The seismic response of buried pipelines is quite complex due to dynamic interactions involving three different components: i) the soil around the structure; ii) the structure itself, depending on geometric and material features; iii) the fluid inside with its specific properties. From a structural point of view, based on the case histories of pipeline damages occurred during the past earthquakes, fragility curves for different kind of lifelines have been developed in the last few years (see, for instance, Lanzano *et al.* 2013) to be used in the context of Na-Tech risk (Natural events triggering Technological disasters) assessments.

Starting from this preface, this paper describes the behavior of onshore pipelines in liquefied soil and the available computational tools for prediction and advanced design, as obtained from a detailed literature survey, providing a general background on this topic. This background is necessary for the design of specific remediation methods (e.g., Mahdi and Katebi 2015, Castiglia *et al.* 2017) to be adopted for the installation of pipelines in soils potentially interested to liquefaction.

2. Liquefaction phenomenon and pipeline buoyancy

Liquefaction is defined as the reduction in effective stress and subsequent loss of stiffness and shear strength, in saturated or nearly saturated soils, due to shaking induced pore water pressure increases. The onset of the phenomenon is currently evaluated, in the professional practice, using methods derived from the well-known Seed and Idriss (1971) approach, as, for instance, the one of Zhang and Goh (2016). Once liquefaction occurs, pore water pressure increases can lead, in some circumstances, buoyancy of

(a)

(b)

Fig. 3 Observed deformation of model before and after shaking (after Sasaki and Tamura 2004)

buried structures. If not properly accounted for, it can result in floatation (Fig. 3) and structural damages. Obviously, this phenomenon is more relevant for relatively light underground structures (i.e., for pipelines transporting natural gas).

Liquefaction happens when the pore water pressure equals the vertical overburden stress, reducing to zero the effective stress state, so that soil behaves like a fluid material. Thus, the buoyant forces resulting from the liquefaction phenomena can be directly related to the depth of pipe burial. The vertical pipe displacement depends on the resisting shear strength in the liquefied soil. The viscous soil creates a drag force that limits the pipe movements. Pipelines that are negatively buoyant with respect to the unit weight of liquefied soil are subject to sinking. Vertical movements due to pipeline buoyancy are generally more significant for large diameter pipelines within soils having relatively low post-liquefied residual strengths. The duration of post-liquefied residual strength is a critical factor in determining total pipe displacement. Pore pressures generated within soils are released, sometimes violently, through the development of cracks, fissures, and spouts. The release can create dynamic pore pressures exceeding the overburden pressures used to define the state of liquefaction. Observations have identified water spouts blowing several meters above the ground surface. Pipes may be subjected to such dynamic pressures and, therefore, specific design procedures are required along the transverse section.

3. Mechanism of floating

The mechanism of flotation can be described referring to the centrifuge tests conducted by Chian *et al.* (2015). Particularly, under static conditions, while the conduit moves upward, soil moves around the edge of the pipe towards the opening cavity beneath the lifting pipe (Fig. 4).

During seismic vibration, excess pore pressure generates

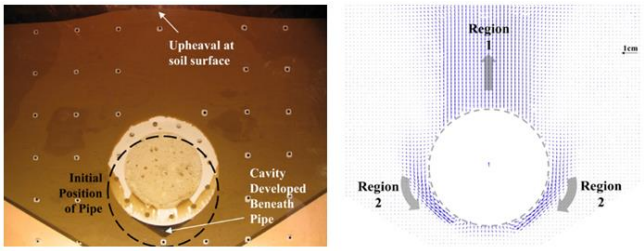

Fig. 4 Static uplift of the pipe in saturated soil (after Chian *et al.* 2015)

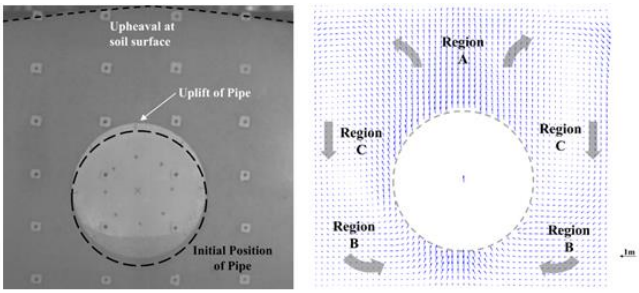

Fig. 5 Dynamic uplift of the pipe in saturated soil (after Chian *et al.* 2015)

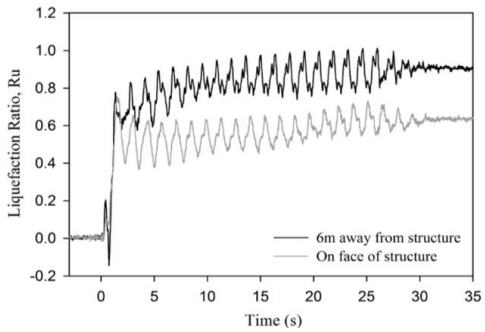

Fig. 6 Liquefaction ratios at the springing depth of the structure and away from it (after Chian *et al.* 2015)

and soil around the pipeline gradually flows in an oval-like trace (Fig. 5).

In fact, due to the low stiffness of the liquefied material, the lifted soil moves laterally away from the structure, as indicated in Region A. At the same time, the soil near the invert of the pipe (Region B) is drawn into the displaced cavity beneath the structure. The soil in Region B is, then, partly replaced by the overlying material (Region C) due to gravity force and constant-volume conditions, which is, in turn, replaced by the soil from Region A. This creates a continuous movement of soil as compared to monotonic uplift, which shows discrete deformation of soil above and adjacent to the structure.

This circular flow is related to the existing of a hydraulic gradient (Fig. 6) for which significant shear at the soil-pipe interface arises from the uplift of the pipe, leading to the dilation of the soil adjacent to it. This results in the recovery of soil stiffness and shear strength in the proximity of the pipe circumference, preventing the migration of the material near the edge of the pipe. This allows also the lower-stiffness liquefied soil, at far field, to flow in a wide loop around this region of dilated soil, in order to fill the expanding cavity beneath the floating pipe. The process

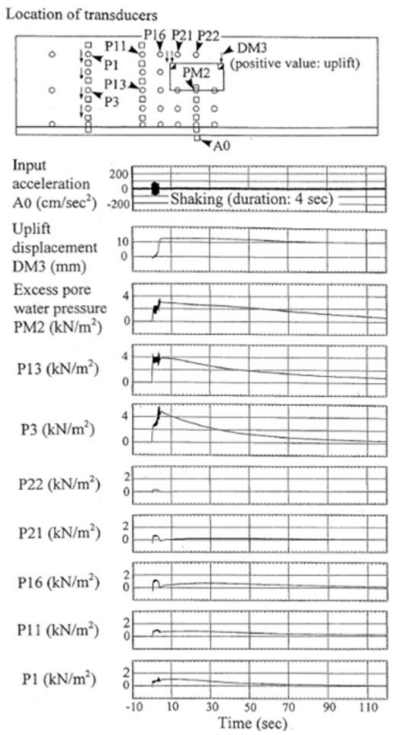

Fig. 7 Shaking table test results (after Koseki *et al.* 1997)

causes both the variation of the effective weight of the overlying soil and the supporting force of soil underlying the pipeline, as well as the shear resistance from shear planes that varies with the degree of liquefaction. The cyclic response of the structure and soil is described, under dynamic conditions, by a 2-D movement.

Definitely, the mechanism of flotation can be summarily represented through the uplift of the buried structure. The uplift initiates, after the application of the shaking, with the generation of excess pore pressure (as indicated, for example, by Huang *et al.* (2014), Sasaki and Tamura (2004) and Chian *et al.* (2014); during shaking, after the soil liquefies, uplift proceeds at nearly constant rate and ceases when shaking stops. The time histories of input acceleration, excess pore water pressures and uplift displacement obtained through shaking table tests conducted by Koseki *et al.* (1997) witnessed this statement, as shown in Fig. 7. Begin and end time of uplifting is highly dependent on the buildup of the excess pore pressure. As expected, a higher uplift is also produced for a shallower buried structure, because of the lower shear resistance and surcharge weight offered by the overlying soil.

4. Computational methods

This part of the paper illustrates the main computational methods that allow individuating the onset of pipeline floatation and the evolution of the process. For easy of understanding, the methods are divided into static and dynamic or advanced approaches.

4.1 Static approaches

Several papers and guidelines (e.g., API 2000, Yu *et al.* 2017) provide insights for the design of embedded pipelines. Design procedures need to be adapted when liquefaction is feared.

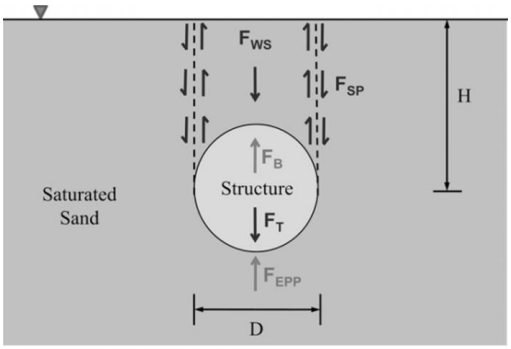

Fig. 8 Force acting on a pipe in liquefied soil (after Chian *et al.* 2014)

Table 1 Soil weights

Soil unit weight	γ (kN/m^3)	19
Soil saturated unit weight	γsat (kN/m^3)	20
Effective soil unit weight	γ' (kN/m^3)	10

Under static conditions, the weight and shear strength of the overlying soil inhibit the flotation. In the event of liquefaction, the soil loses most of its shear strength, and the structure may float as a result. Factor affecting floatation can be simply understand looking at Fig. 8. The problem can be analyzed considering a simple equilibrium at the vertical translation that involves weights, shear resistance and uplift forces.

Key points are the role of soil above the pipe and its interaction with the surrounding soils, and the development of pore water pressure.

According to Chian *et al.* (2014) and Koseki *et al.* (1997), the safety factor against uplift, Fs, can be computed using the Eq. (1) where F_T is the weight of the structure, F_{SP} is the frictional resistance force which is proportional to the shear strength of the soil and the buried depth of the structure, F_{WS} is the weight of the overlying soil layer that represents a surcharge acting on the structure, F_B is the buoyant force due to hydrostatic pressure and to excess pore water pressure caused by soil liquefaction, and F_{EPP} is the seepage force transferred from the soil underlying the structure. The latter component should be considered only when a relatively large amount of excess pore water pressure is generated at a deeper portion of the underlying soil. Consequently, the uplift force, F_{NET}, can be calculated from the Eq. (2).

$$F_s = \frac{F_T + F_{SP} + F_{WS}}{F_B + F_{EPP}} \tag{1}$$

$$F_{NET} = \left(F_B + F_{EPP}\right) - \left(F_T + F_{SP} + F_{WS}\right) \tag{2}$$

On the safer side, if the soil is completely liquefied, the buoyancy force can be calculated from the unit weight of the saturated soil; if the soil partially liquefies, buoyancy can be defined as a resultant force of the total stresses

Table 2 Weight of the overlying soil F_{ws} and buoyant force F_B values for different depth and pipeline diameter

			H (m)							Soil completely liquefied	Soil partially liquefied
			0.9	1	1.1	1.2	1.3	1.4	1.5		
Size	D (m)	V (m^3)	F_{ws} (kN)	F_{ws} (kN)	F_{ws} (kN)	F_{ws} (kN)	F_{ws} (kN)	F_{ws} (kN)	F_{ws} (kN)	F_B (kN)	F_B (kN)
30	0.762	0.456	4.58	5.34	6.10	6.86	7.63	8.39	9.15	9.121	4.56
32	0.813	0.519	4.72	5.53	6.35	7.16	7.97	8.79	9.60	10.382	5.19
34	0.864	0.586	4.84	5.71	6.57	7.44	8.30	9.16	10.03	11.726	5.86
36	0.914	0.656	4.95	5.86	6.77	7.69	8.60	9.52	10.43	13.122	6.56
38	0.965	0.731	5.03	5.99	6.96	7.92	8.89	9.85	10.82	14.628	7.31
40	1.016	0.811	5.09	6.11	7.12	8.14	9.15	10.17	11.19	16.215	8.11
42	1.067	0.894	5.13	6.20	7.27	8.33	9.40	10.47	11.53	17.883	8.94
44	1.118	0.982	5.15	6.27	7.39	8.51	9.63	10.74	11.86	19.634	9.82
46	1.168	1.071	5.15	6.32	7.49	8.66	9.83	10.99	12.16	21.429	10.71
48	1.219	1.167	5.14	6.35	7.57	8.79	10.01	11.23	12.45	23.341	11.67
52	1.321	1.371	5.04	6.36	7.68	9.00	10.32	11.64	12.96	27.411	13.71
56	1.422	1.588	4.86	6.28	7.70	9.12	10.55	11.97	13.39	31.763	15.88
60	1.524	1.824	4.60	6.12	7.64	9.17	10.69	12.22	13.74	36.483	18.24

Table 3 Weight of the structure F_T and safety factor against uplift F_S values for different pipeline diameter, thickness and burial depth

						H (m)							H (m)					
						0.9	1	1.1	1.2	1.3	1.4	1.5	0.9	1	1.1	1.2	1.3	1.4	1.5
Size	D (m)	t (m)	D/t	W (kN/m)	F_T (kN)	F_S							F_S						
30	0.762	0.0079	96.46	1.47	1.469	0.66	0.75	0.83	0.91	1.00	1.08	1.16	1.33	1.49	1.66	1.83	1.99	2.16	2.33
		0.0087	87.59	1.62	1.616	0.68	0.76	0.85	0.93	1.01	1.10	1.18	1.36	1.53	1.69	1.86	2.03	2.19	2.36
		0.0095	80.21	1.76	1.763	0.70	0.78	0.86	0.95	1.03	1.11	1.20	1.39	1.56	1.72	1.89	2.06	2.23	2.39
		0.0103	73.98	1.91	1.909	0.71	0.79	0.88	0.96	1.05	1.13	1.21	1.42	1.59	1.76	1.92	2.09	2.26	2.43
		0.0111	68.65	2.06	2.055	0.73	0.81	0.89	0.98	1.06	1.14	1.23	1.45	1.62	1.79	1.96	2.12	2.29	2.46
		0.0119	64.03	2.20	2.201	0.74	0.83	0.91	0.99	1.08	1.16	1.24	1.49	1.65	1.82	1.99	2.15	2.32	2.49
		0.0127	60.00	2.35	2.347	0.76	0.84	0.93	1.01	1.09	1.18	1.26	1.52	1.69	1.85	2.02	2.19	2.35	2.52
		0.0143	53.29	2.64	2.637	0.79	0.87	0.96	1.04	1.13	1.21	1.29	1.58	1.75	1.92	2.08	2.25	2.42	2.58
		0.0159	47.92	2.93	2.925	0.82	0.91	0.99	1.07	1.16	1.24	1.32	1.65	1.81	1.98	2.15	2.31	2.48	2.65
		0.0175	43.54	3.21	3.213	0.85	0.94	1.02	1.10	1.19	1.27	1.36	1.71	1.88	2.04	2.21	2.38	2.54	2.71
		0.0191	39.90	3.50	3.499	0.89	0.97	1.05	1.14	1.22	1.30	1.39	1.77	1.94	2.11	2.27	2.44	2.61	2.77
		0.0206	36.99	3.77	3.766	0.91	1.00	1.08	1.17	1.25	1.33	1.42	1.83	2.00	2.16	2.33	2.50	2.67	2.83
		0.0222	34.32	4.05	4.050	0.95	1.03	1.11	1.20	1.28	1.36	1.45	1.89	2.06	2.23	2.39	2.56	2.73	2.89
		0.0238	32.02	4.33	4.333	0.98	1.06	1.14	1.23	1.31	1.39	1.48	1.95	2.12	2.29	2.46	2.62	2.79	2.96
		0.0254	30.00	4.61	4.614	1.01	1.09	1.17	1.26	1.34	1.43	1.51	2.02	2.18	2.35	2.52	2.68	2.85	3.02
		0.0270	28.22	4.89	4.894	1.04	1.12	1.21	1.29	1.37	1.46	1.54	2.08	2.24	2.41	2.58	2.75	2.91	3.08
		0.0286	26.64	5.17	5.173	1.07	1.15	1.24	1.32	1.40	1.49	1.57	2.14	2.31	2.47	2.64	2.81	2.97	3.14
		0.0302	25.23	5.45	5.450	1.10	1.18	1.27	1.35	1.43	1.52	1.60	2.20	2.37	2.53	2.70	2.87	3.03	3.20
		0.0318	23.96	5.73	5.726	1.13	1.21	1.30	1.38	1.46	1.55	1.63	2.26	2.43	2.59	2.76	2.93	3.09	3.26
									H (m)								H (m)		
						0.9	1	1.1	1.2	1.3	1.4	1.5	0.9	1	1.1	1.2	1.3	1.4	1.5
Size	D (m)	t (m)	D/t	W (kN/m)	F_T (kN)	F_S							F_S						
42	1.067	0.0111	96.13	2.89	2.890	0.45	0.51	0.57	0.63	0.69	0.75	0.81	0.90	1.02	1.14	1.26	1.37	1.49	1.61
		0.0119	89.66	3.10	3.096	0.46	0.52	0.58	0.64	0.70	0.76	0.82	0.92	1.04	1.16	1.28	1.40	1.52	1.64

Table 3 Continued

						H (m)													
						0.9	1	1.1	1.2	1.3	1.4	1.5	0.9	1	1.1	1.2	1.3	1.4	1.5
Size	D (m)	t (m)	D/t	W (kN/m)	F_T (kN)	F_S							F_S						
		0.0127	84.02	3.30	3.302	0.47	0.53	0.59	0.65	0.71	0.77	0.83	0.94	1.06	1.18	1.30	1.42	1.54	1.66
		0.0143	74.62	3.71	3.712	0.49	0.55	0.61	0.67	0.73	0.79	0.85	0.99	1.11	1.23	1.35	1.47	1.59	1.71
		0.0159	67.11	4.12	4.121	0.52	0.58	0.64	0.70	0.76	0.82	0.88	1.03	1.15	1.27	1.39	1.51	1.63	1.75
		0.0175	60.97	4.53	4.529	0.54	0.60	0.66	0.72	0.78	0.84	0.90	1.08	1.20	1.32	1.44	1.56	1.68	1.80
		0.0191	55.86	4.94	4.936	0.56	0.62	0.68	0.74	0.80	0.86	0.92	1.13	1.25	1.36	1.48	1.60	1.72	1.84
		0.0206	51.80	5.32	5.316	0.58	0.64	0.70	0.76	0.82	0.88	0.94	1.17	1.29	1.41	1.53	1.65	1.77	1.88
		0.0222	48.06	5.72	5.720	0.61	0.67	0.73	0.79	0.85	0.91	0.96	1.21	1.33	1.45	1.57	1.69	1.81	1.93
		0.0238	44.83	6.12	6.123	0.63	0.69	0.75	0.81	0.87	0.93	0.99	1.26	1.38	1.50	1.62	1.74	1.86	1.97
		0.0254	42.01	6.52	6.524	0.65	0.71	0.77	0.83	0.89	0.95	1.01	1.30	1.42	1.54	1.66	1.78	1.90	2.02
		0.0270	39.52	6.92	6.925	0.67	0.73	0.79	0.85	0.91	0.97	1.03	1.35	1.47	1.59	1.71	1.83	1.95	2.06
		0.0286	37.31	7.32	7.324	0.70	0.76	0.82	0.88	0.94	0.99	1.05	1.39	1.51	1.63	1.75	1.87	1.99	2.11
		0.0302	35.33	7.22	7.221	0.69	0.75	0.81	0.87	0.93	0.99	1.05	1.38	1.50	1.62	1.74	1.86	1.98	2.10
		0.0318	33.55	8.12	8.118	0.74	0.80	0.86	0.92	0.98	1.04	1.10	1.48	1.60	1.72	1.84	1.96	2.08	2.20

						H (m)													
						0.9	1	1.1	1.2	1.3	1.4	1.5	0.9	1	1.1	1.2	1.3	1.4	1.5
Size	D (m)	t (m)	D/t	W (kN/m)	F_T (kN)	F_S							F_S						
60	1.524	0.0159	95.85	5.91	5.913	0.29	0.33	0.37	0.41	0.46	0.50	0.54	0.58	0.66	0.74	0.83	0.91	0.99	1.08
		0.0175	87.09	6.90	6.901	0.32	0.36	0.40	0.44	0.48	0.52	0.57	0.63	0.71	0.80	0.88	0.96	1.05	1.13
		0.0191	79.79	7.09	7.088	0.32	0.36	0.40	0.45	0.49	0.53	0.57	0.64	0.72	0.81	0.89	0.97	1.06	1.14
		0.0206	73.98	7.64	7.637	0.34	0.38	0.42	0.46	0.50	0.54	0.59	0.67	0.75	0.84	0.92	1.00	1.09	1.17
		0.0222	68.65	8.22	8.222	0.35	0.39	0.43	0.48	0.52	0.56	0.60	0.70	0.79	0.87	0.95	1.04	1.12	1.20
		0.0238	64.03	8.80	8.805	0.37	0.41	0.45	0.49	0.53	0.58	0.62	0.73	0.82	0.90	0.99	1.07	1.15	1.24
		0.0254	60.00	9.39	9.387	0.38	0.43	0.47	0.51	0.55	0.59	0.63	0.77	0.85	0.93	1.02	1.10	1.18	1.27
		0.0270	56.44	9.97	9.967	0.40	0.44	0.48	0.52	0.57	0.61	0.65	0.80	0.88	0.97	1.05	1.13	1.22	1.30
		0.0286	53.29	10.55	10.547	0.42	0.46	0.50	0.54	0.58	0.62	0.67	0.83	0.91	1.00	1.08	1.16	1.25	1.33
		0.0302	50.46	11.12	11.125	0.43	0.47	0.51	0.56	0.60	0.64	0.68	0.86	0.95	1.03	1.11	1.20	1.28	1.36
		0.0318	47.92	11.70	11.702	0.45	0.49	0.53	0.57	0.61	0.66	0.70	0.89	0.98	1.06	1.14	1.23	1.31	1.39

acting on the entire surface of the structure, determined by the pore water pressure and the effective stress of the soil. In both cases, no tangential forces due to the potential vertical movement of the system should be considered, because of the loss of shear strength induced in the soil by liquefaction.

Assuming the ground water level at the ground surface, the soil weights of Table 1, and neglecting the seepage forces, in the following the safety factor values for buried pipeline in completely and partially liquefied soils have been calculated, referring to the American Petroleum Institute Specification for line pipe in terms of diameters and weights (API Specification 2002).

Particularly, the study refers to all diameters and thickness and to all burial depths usually adopted for pipeline systems and interesting for liquefaction problems, which is to say:

• Burial depths range between 0.9-1.5m (greater depths are used only in special cases);

• Diameters greater than 0.75 m;

• Diameter/thickness ratio ranging from about 15 to 100.

If D is the pipeline diameter, t its thickness, W its weight per unit length, V the volume of the pipe transverse section and H the depth of the center of the pipe from the ground level, F_{ws} for each considered burial depths and F_B in case of completely or partially liquefied soil are available in Table 2. F_T for each pipe thickness and the safety factors values for each burial depth are provided in Table 3, considering a unitary longitudinal length of the pipe and three specific pipe sizes as for example (i.e., small 30", medium 42", and large diameter 60"). For the purpose of this analysis, pipelines are considered empty. The pipeline is assumed to be in equilibrium for a unitary safety factor.

From the analysis of the safety factor values, it can be highlighted how, for partially liquefiable soil conditions (in which the buoyancy force has been calculated through the effective soil unit weight), the stability against pipeline

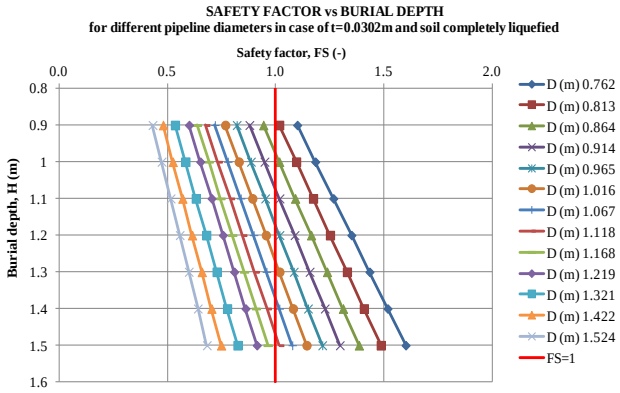

Fig. 9 Safety factor vs burial depth

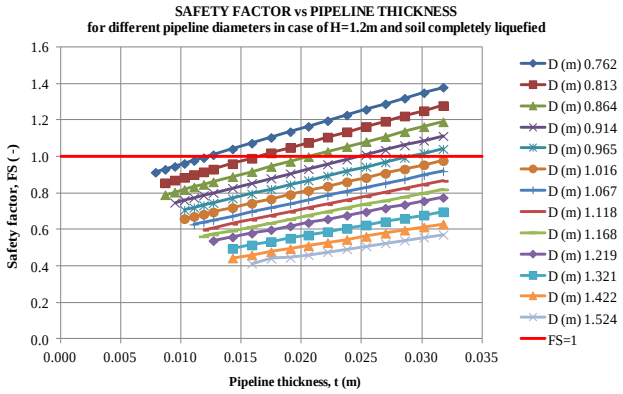

Fig. 10 Safety factor vs pipeline thickness

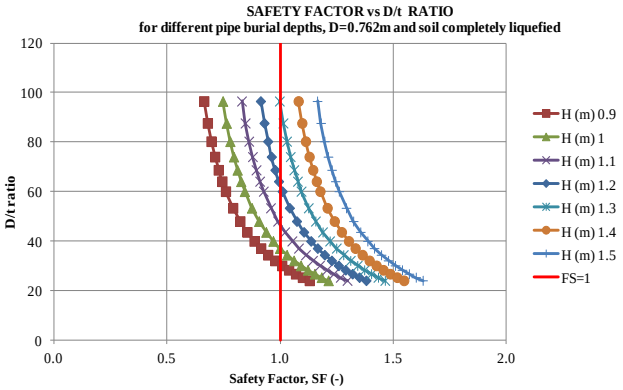

Fig. 11 Safety factor vs D/t ratio

flotation can be ensured, except for bigger diameters (D>1 m), shallow burial depths and small thickness (consequently small pipe weight). However, for completely liquefiable soils, problems soon arise in case of small diameters and shallow burial depths, in a more pronounced way as the thickness increases. Furthermore, the safety factor is never equal or greater than one for diameters exceeding 1.150 m, and is equal to one for smaller diameters (up to 1 m) just in few cases of high burial depths and major thickness.

Fig. 9 shows the relationship between the safety factors and the burial depths for a large variety of pipeline diameters, referring to a thickness value of 0.0302 m in the case of completely liquefiable soils. Safety factor values increase with increasing depth, in a similar way for each diameter (lines are almost parallel), with higher values for small ones. This is in accordance with the higher pipelines volumes for bigger diameters, which lead to an increase in the buoyancy forces, while soil weight is almost the same (the burial depth decreases but the diameter increases so the soil volume does not change significantly).

Fig. 10 depicts how the safety factor changes by varying the pipe thickness, for the different diameters, fixing a burial depth of 1.2 m and considering the complete liquefaction of soil. Safety factor increases with increasing pipe thickness as the diameter decreases. Being valid the same aforementioned considerations, for greater thickness the pipeline weight increases, increasing the equilibrium resistance force.

The last example is in Fig. 11, where the safety factor is expressed in relation to the D/t ratio and increases in decreasing the ratio and in increasing the burial depth. This case refers to completely liquefiable soils too and to D=0.762 m and confirms the previously remarks.

4.2 Advanced approaches

To study the behavior of pipelines in liquefied soils under dynamic conditions, experiments such as centrifuge or shaking table tests are often required.

This kind of experimentation allows reproducing the real soil configuration in situ and is the most direct and effective approach to analyze the problem in a reduced scale. These tests usually provide acceleration time histories at selected locations of the model, the development of excess pore water with time at different positions (i.e., near and far to the structure), soil deformations and soil-structure interaction response. However, the equipment is very expensive and often the interpretation of the test results is obtained through numerical analyses.

In this paragraph, the main advanced procedures applied to study the behaviour of a buried structure in liquefiable soils will be shown, looking at the key results obtained and the main limitations of the methods.

Chian *et al.* (2014) carried out numerical analyses using the FLAC code (Fig. 12(a)). The Authors used a nonlinear, fully coupled bounding surface plasticity constitutive model for sand obtained by Wang (1990), which is specifically formulated to capture the contraction and dilation induced by cyclic shear stresses. The numerical analysis match very well with centrifuge test results far from the structure, but it is not able to study soil-structure interaction satisfactorily, because of the meshing scheme, as shown in the comparison between excess pore-pressure time histories around the structure obtained from experimental and numerical analysis in Fig. 12(b).

Ling *et al.* (2008) used a coupled stress-flow finite element procedure with DIANA-SWANDYNE II code, a unified general-purpose 2-D program, where the soil was modeled by the Pastor-Zienkiewicz Mark-III scheme referring to Pastor *et al.* (1990). The acceleration, excess pore pressure and uplifting of the pipe were well simulated by the finite element procedure up to the stage of liquefaction, but difficulties were encountered in modeling the post-liquefaction behavior (Fig. 13). This was because of the inability to reproduce soil-structure interaction, which led to the development of tensions in the soil elements around the bottom of the pipe affecting results, and because

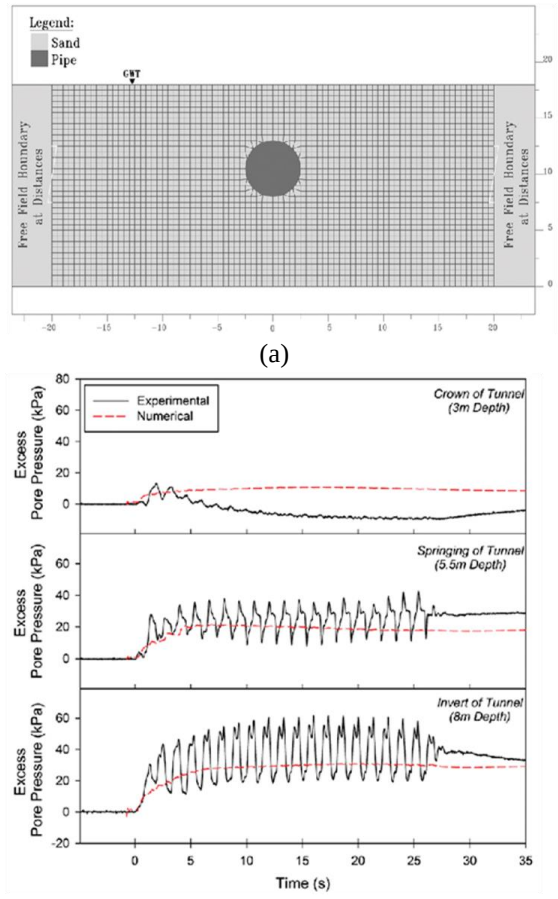

Fig. 12 Numerical layout (a) dimensions in meters) and comparison between experimental and numerical analysis results (b) (Chian *et al.* 2014)

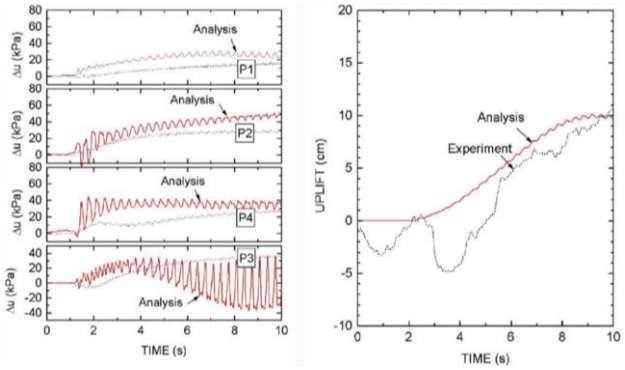

Fig. 13 Excess pore water pressure around pipe and pipe uplifting (Ling *et al.* 2008)

of the small-strain finite element procedure, which did not allow analyzing large deformations, such as uplifting of the pipe.

Some other studies referred to the analysis of underground structures different from pipelines but they can be used to highlight some specific features.

Liu and Song (2005) used the 2-D, effective-stress based, fully coupled dynamic finite element code DYNA Swandyne-II too. They investigated the dynamic behavior of a subway station in saturated sandy deposit (some results are in Fig. 14).

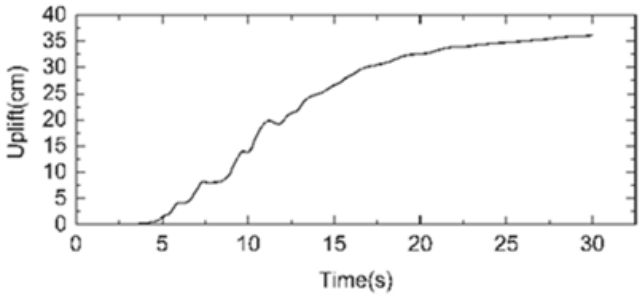

(a) The relationship between the uplifting amount with time

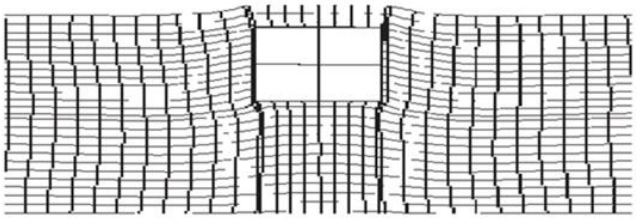

(b) Part of the deformed mesh (Enlarged five times)

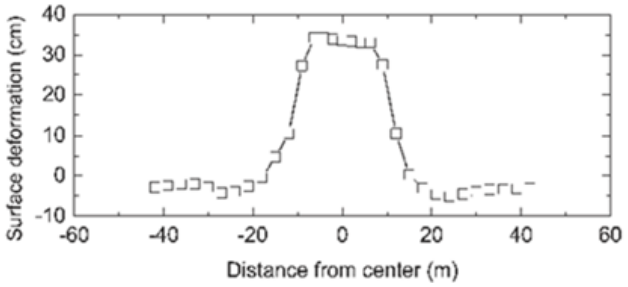

(c) Ground surface deformation

Fig. 14 Uplift of the underground structure obtained by Liu and Song (2005)

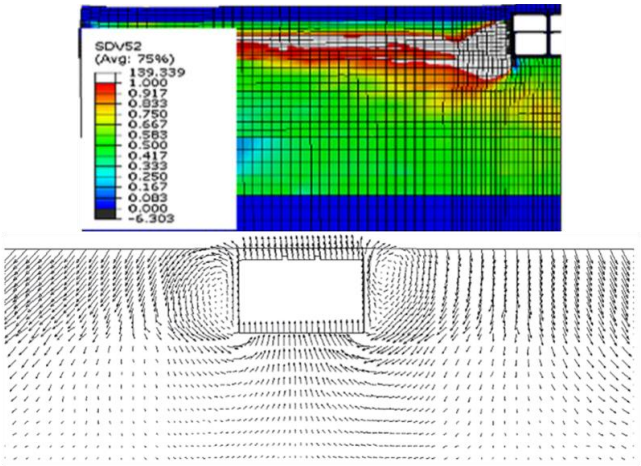

Fig. 15 Dynamic pore pressure ratio and displacement vectors around the underground structure with ABAQUS (Zhuang *et al.* 2015)

For the analysis, the non-associated generalized plasticity model of Ling *et al.* (2003) with 15 parameters was used. This model is capable of simulating cyclic liquefaction, cyclic hardening and pressure dependency of sandy soil and is aimed at reproducing the behavior of sands under monotonic and cyclic loadings at different mean effective stress levels. The analysis was carried on considering the soil–structure interface through a SLIP

ELEMENT III material model, which can describe the slippage of interfaces simulating the separation and closure behavior and allows the simulation of considerable displacements. From the numerical analyses, the following conclusions were obtained: the presence of the underground structure caused the value of excess pore water pressure to be modified; the heaving of the ground surface was smaller than the uplift amount of the underground structure, indicating deformation of the soil on top of the structure due to earthquake-induced liquefaction; and, the increase of the buried depth improved the safety.

Zhuang *et al.* (2015) used the general-purpose 2D finite element program Abaqus to study the response of a subway station. To simulate the liquefied-induced large deformation of the ground, they used an arbitrary Lagrangian-Eulerian (ALE) adaptive meshing method, thus maintaining a high-quality mesh system for the soil throughout the analysis process when large deformations or losses of soil occurred, allowing the mesh to move independently. The advanced numerical model reported in Yang (2000) was used to reproduce the nonlinear static and dynamic coupling interactions between the liquefiable ground and the underground structure. One example of the analyses results is shown in Fig. 15.

Overall, a large number of centrifuge shaking table tests were performed during last years, allowing understanding the behavior of liquefied soil and of buried structures. In addition, numerous analyses with different computational codes, soil constitutive models specifically chosen to best simulate soil behavior in the case of liquefaction, proper contour conditions both around the structure and at the edge of the model were conducted giving generally satisfactorily results. However, simple and easy to handle constitutive models capable of describing exhaustively liquefaction phenomena during and after earthquake excitation seem not to exist nowadays. A large number of parameters and very complex mathematical formulations characterizes the soil constitutive models usually employed. Moreover, the need to capture soil-structure interaction remains a problem because of the meshing scheme: FEM suffers several disadvantages because of mesh tangling, even when the updated Lagrangian method is adopted. The adaptive meshing method solves partially the problem of large deformations but the procedure is quite complicated. These main aspects require big computational efforts and the post-liquefaction response remains a challenge to date with conventional numerical methods.

5. SPH approach

Over the last few years, the Smoothed Particle Hydrodynamics (SPH) method has been extended to a wide range of problems in both fluid and solid mechanics because of its strong ability to incorporate complex physical concepts into a unique formulation. A variety of SPH models have been proposed and applied to specific topics in geo-disasters too, including dam breaks and coastal engineering, flow-like landslides, the lateral spread of liquefied soil, seepage failure, dynamic erosion, underground explosions and rock breakage (Maeda *et al.* 2006, Bui *et al.* 2008, Pastor *et al.* 2009, Shao 2010, Bui *et al.* 2011, Stefanova *et al.* 2012, Dai *et al.* 2014, Ibrahim 2015, Koneshwaran *et al.* 2015). In the following, there are some interesting examples on the SPH method applications. The first one refers to a numerical simulation of the seepage process around a sheet pile (Fig. 16), with particular attention to (a) the initial condition, (b) the yield of base surface on downstream side and the sinking on upstream

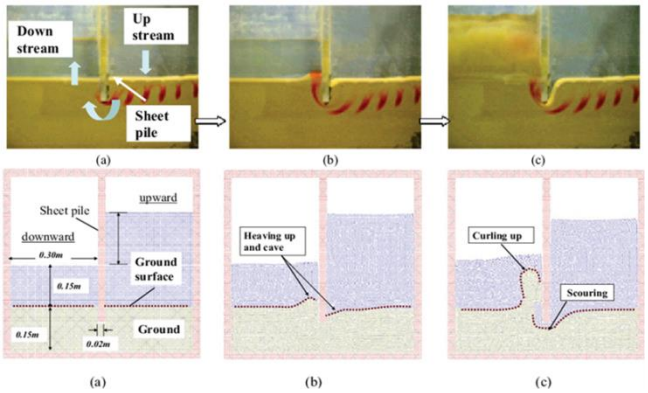

Fig. 16 Seepage failure around sheet pile simulation with SPH (Maeda *et al.* 2006)

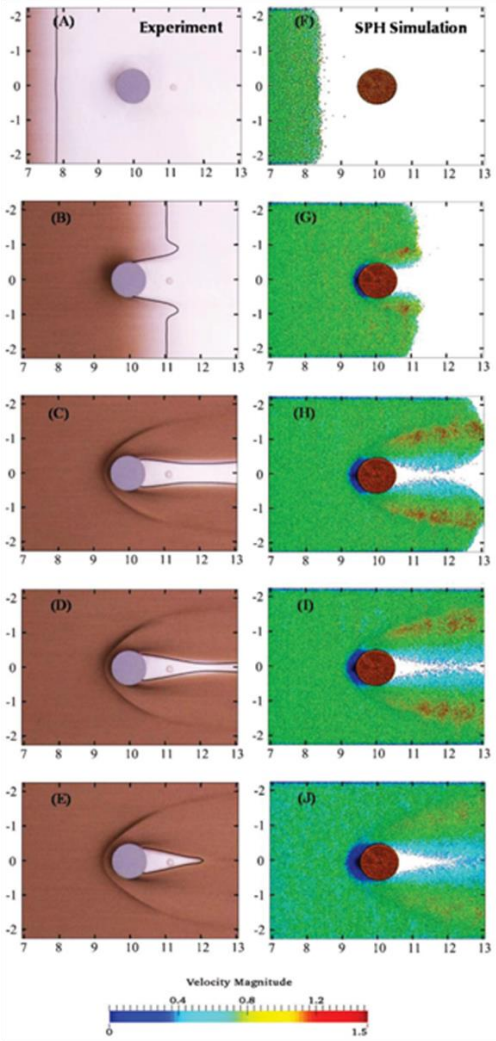

Fig. 17 Simulation of a granular flow passing an obstacle through SPH (Ibrahim 2015)

side, and (c) failure: curling up and scour.

The results of the simulation are shown together with the experimental ones, thus allowing a comparison, which results in a good simulation of the seepage failure in soil. This is an important tool, considering that large-scale deformation and hydraulic collapse of the ground, induced by water flow through the ground, plays a significant role in the destabilization of dam foundations during floods, liquefaction and other catastrophic events.

The second example shows a comparison between computation and experiment results at different time steps, simulating the continuation of the time-dependent development of a bow shock and a vacuum boundary (Fig. 17).

From the achievements of the studies here just recalled, the SPH method has significant advantages over traditional grid-based numerical modeling when dealing with geo-disasters as reported by Huang and Dai (2014):

• SPH is suitable for problems where the material is not a continuum, indeed objects are discretized into a series of particles without using a grid/mesh;

• As particle method, it can process larger local distortion because the connectivity between the particles is generated as part of the computation and can change with time, so that just an initial discretization is required and the refinement of particles would be much easier to perform than the mesh refinement, even for complex geometries;

• As a Lagrangian method, a SPH code is conceptually simpler than grid-based methods and should be faster as no convective term exists in the related partial differential equations;

• The motion of the particles can be traced and the features of the entire physical system can be easily obtained. Therefore, it is easier to identify the free surfaces, moving interfaces, and deformable boundaries using SPH than by Eulerian methods. The time history of the field variables at each material point can also be obtained in the simulation;

• SPH guarantees conservation of mass without extra computation since the particles themselves represent mass. Pressure is computed from the weighted contributions of the neighboring particles rather than by solving the linear systems of equations;

• SPH allows the study of the behavior and interaction of different materials (fluid, solids) and offers the capability to include multiphase soil models.

Despite these good performances, SPH still suffers from a number of shortcomings:

• Imprecision caused by the lack of particle coverage near boundaries;

• Tensile instability when handling problems with material strength;

• Zero-energy modes when field variables and their derivatives are calculated at the same locations;

• In addition, 3D analysis approach, generally used for a more realistic simulation, requires many particles throughout the SPH region, and being a computationally intensive numerical method, it needs extensive computer memory and longer computational run times.

The technique of producing hybrid mixes of different numerical methods is also possible (Wang *et al*. 2005, Holz *et al.* 2009), thus improving computing efficiency and extending the application of both methods.

Concerning liquefaction simulations, there are not substantial studies up to now, but just few cases of lateral spread and flow mechanism (Naili *et al*. 2005a, Naili *et al.* 2005b, Huang *et al.* 2011, Huang *et al*. 2013), none of them including the soil-structure interaction. The absence of simulation of complete case-histories of soil-structure interaction in case of liquefaction using the SPH approach is maybe due to the relatively young approach, which is still not assessed at all and still used for simple simulations. However, recently new approaches for modeling the boundary between soil and structures in the framework of SPH approach are developing, (see, for instance, Niroumand *et al.* 2016), thus indicating the possibility to join in the near future knowledges derived from the soil-structure interaction framework and soil liquefaction behavior using particles or coupled methods. Therefore, looking at the other successfully applications of the method, this would be an important tool to deepen improving numerical results.

6. Conclusions

Liquefaction is a soil failure phenomenon, which occurs under site-specific condition (loose saturated soils, high seismic hazard), compatible to many coastal and fluvial flat lands where usually onshore pipelines and plants are located. Based on field post-earthquake observations, this phenomenon represents a crucial issue for the risk assessment of industrial components and lifelines. In this paper, we recalled the main relevant aspects of the seismic hazard of buried pipelines and the soil-structure interaction in case of liquefaction. The problem of flotation affects the behavior of a buried pipeline in the vertical transverse section, when the liquefaction phenomenon occurs, because of the development of excess pore water pressure in the soil surrounding the pipe. This problem requires specific remedial. The onset of floating of the buried structure is associated to the unit value of a computed safety factor that is, generally, evaluated in static conditions employing very simple formulation of vertical equilibrium. However, to consider all the main aspects of the phenomenon, advanced analyses should be processed. In this field, soil exhibits very complicated behavior under seismic loading, so that it is quite difficult to reproduce the complete behavior of embedded pipelines through FEM numerical analyses. New kinds of analysis could be investigated and experimental tests are required. In this paper, we clarified the mechanism of flotation and we pictured the state of the art on computational methods reproducing soil-structure interaction in case of liquefaction, providing an overview of the numerical codes, constitutive models and procedures, underlining their main limitations. Finally, we reminded a new approach for a method recently adopted in geo-disaster field, named Smoothed Particle Hydrodynamics SPH.

Acknowledgments

This research was developed in the framework of an

agreement between the University of Molise, Italy and Saipem S.p.A. The support of Mr. Salvatore Morgante and Mr. Filippo Onori, Saipem S.p.A., is deeply acknowledged.

References

API Specification (2000), *Specification for Line Pipe*, American Petroleum Institute.

Bui, H.H., Fukagawa, R., Sako, K. and Wells, J.C. (2011), "Slope stability analysis and discontinuous slope failure simulation by elasto-plastic smoothed particle hydrodynamics (SPH)", *Géotechnique*, **61**(7), 565-574.

Bui, H.H., Sako, K., Fukagawa, R. and Wells J.C. (2008), "SPH-based numerical simulations for large deformation of geomaterial considering soil-structure interaction", *Proceedings of the 12th International Conference of International Association for Computer Methods and Advances in Geomechanics*, Goa, India, October.

Castiglia, M., Morgante, S., Napolitano, A. and Santucci de Magistris, F. (2017), "Mitigation measures for the stability of pipelines in liquefiable soils", *J. Pipeline Eng.*, **16**(3), 115-139.

Chian, S.C., Tokimatsu, K. and Madabhushi, S.P.G. (2014), "Soil liquefaction-induced uplift of underground structures: Physical and numerical modeling", *J. Geotech. Geoenviron. Eng.*, **140**(10), 04014057.

Chian, S.C., Wang, J., Haigh, S.K. and Madabhushi, S.P.G. (2015), "Soil deformation during monotonic and seismic pipe uplift in liquefiable soil", *J. Pipeline Eng.*, **14**(1), 33-41.

Dai, Z., Huang, Y., Cheng, H. and Xu, Q. (2014), "3D numerical modeling using smoothed particle hydrodynamics of flow-like landslide propagation triggered by the 2008 Wenchuan earthquake", *Eng. Geol.*, **180**, 21-33.

GEER (2010), *Geo-Engineering Reconnaissance of the February 27, 2010 Maule, Chile Earthquake*, Geoengineering Extreme Events Reconnaissance GEER Association Report No. GEER-022 Version 2: May 25, 2010

Holz, D., Beer, T. and Kuhlen, T. (2009), *Soil Deformation Models for Real-Time Simulation: A Hybrid Approach*, in *Workshop on Virtual Reality Interaction and Physical Simulation VRIPHYS*.

Huang, B., Liu, J., Lin, P. and Ling, D. (2014), "Uplifting behavior of shallow buried pipe in liquefiable soil by dynamic centrifuge test", *Sci. World J.*

Huang, Y. and Dai, Z. (2014), "Large deformation and failure simulations for geo-disasters using smoothed particle hydrodynamics method", *Eng. Geol.*, **168**, 86-97.

Huang, Y., Zhang, W., Dai, Z. and Xu, Q. (2013), "Numerical simulation of flow processes in liquefied soils using a soil-water-coupled smoothed particle hydrodynamics method", *Nat. Hazards*, **69**(1), 809-827.

Huang, Y., Zhang, W.J., Mao, W.W. and Jin, C. (2011), "Flow analysis of liquefied soils based on smoothed particle hydrodynamics", *Nat. Hazards*, **59**(3), 1547-1560.

Ibrahim, A.M.A. (2015), "Modeling and analysis of geo-disaster problems using the SPH method", Ph.D. Dissertation, Hokkaido University, Hokkaido, Japan.

Kazem, S., Shokouhi, S., Dolatshah, A. and Ghobakhloo, E. (2013), "Seismic strain analysis of buried pipelines in a fault zone using hybrid FEM-ANN approach", *Earthq. Struct.*, **5**(4), 417-438.

Koneshwaran, S., Thambiratnam, D.P. and Gallage C. (2015), "Blast response of segmented bored tunnel using coupled SPH-FE method", *Struct.*, **2**, 58-71.

Koseki, J., Matsuo, O. and Koga Y. (1997), "Uplift behavior of underground structures caused by liquefaction of surrounding soil during earthquake", *Soil. Found.*, **37**(1), 97-108.

Lanzano, G., Salzano, E., Santucci de Magistris, F. and Fabbrocino, G. (2013), "Seismic vulnerability of natural gas pipelines", *Reliab. Eng. Syst. Safe.*, **117**, 73-80.

Lanzano, G., Santucci de Magistris, F., Fabbrocino, G. and Salzano, E. (2015), "Seismic damage to pipelines in the framework of Na-Tech risk assessment", *J. Loss Prevent. Proc. Industr.*, **33**, 159-172.

Ling, H.I., Mohri, Y., Kawabata, T., Liu, H., Burke, C. and Sun L. (2003), "Centrifugal modeling of seismic behavior of large-diameter pipe in liquefiable soil", *J. Geotech. Geoenviron. Eng.*, **129**(12), 1092-1011.

Ling, H.I., Sun, L., Liu, H., Mohri, Y. and Kawabata T. (2008), "Finite element analysis of pipe buried in saturated soil deposit subject to earthquake loading", *J. Earthq. Tsunami*, **2**(1), 1-17.

Liu, H. and Song, E. (2005), "Seismic response of large underground structures in liquefiable soils subjected to horizontal and vertical earthquake excitations", *Comput. Geotech.*, **32**(4), 223-244.

Maeda, K., Sakai, H. and Sakai M. (2006), "Development of seepage failure analysis method of ground with smoothed particle hydrodynamics", *Struct. Eng. Earthq. Eng.*, **23**(2), 307-319.

Mahdi, M. and Katebi, H. (2015), "Numerical modeling of uplift resistance of buried pipelines in sand, reinforced with geogrid and innovative grid-anchor system", *Geomech. Eng.*, **9**(6), 757-774.

Naili, M., Matsushima, T. and Yamada, Y. (2005a), "A 2D smoothed particle hydrodynamics method for liquefaction induced lateral spreading analysis", *Journal of Applied Mechanical*, **8**, 591–599.

Naili, M., Matsushima, T. and Yamada, Y. (2005b), "Smoothed particles hydrodynamics for numerical simulation of soil-structure problem due to liquefaction", *Proceedings of the 40th Japan National Conference on Geotechnical Engineering*, Hokkaido, Japan, July.

Niroumand, H., Mehrizi, M.E.M. and Saaly, M. (2016), "Application of mesh-free smoothed particle hydrodynamics (SPH) for study of soil behavior", *Geomech. Eng.*, **11**(1), 1-39.

O'Rourke, M.J. and Liu, X. (1999), *Response of Buried Pipelines Subjected to Earthquake Effects*, MCEER Monograph No.3, University of New York, Buffalo, New York, U.S.A.

Paolucci, R., Griffini, S. and Mariani, S. (2010), "Simplified modelling of continuous buried pipelines subject to earthquake fault rupture", *Earthq. Struct.*, **1**(3), 253-267.

Pastor, M., Haddad, B., Sorbino, G. and Drempetic V. (2009), "A depth-integrated, coupled SPH model for flow-like landslides and related phenomena", *J. Numer. Anal. Meth. Geomech.*, **33**(2), 143-172.

Pastor, M., Zienkiewicz, O.C. and Chan, A.H.C. (1990), "Generalized plasticity and the modeling of soil behavior", *J. Numer. Anal. Meth. Geomech.*, **14**(3), 151-190.

Sasaki, T. and Tamura, K. (2004), "Prediction of liquefaction-induced uplift displacement of underground structures", *Proceedings of the 36th Joint Meeting U.S.-Japan Panel on Wind and Seismic Effects*, Gaithersburg, Maryland, U.S.A.

Seed, H.B. and Idriss, I.M. (1971), "Simplified procedure for evaluating soil liquefaction potential", *J. Soil Mech. Found. Div.*, **97**(9), 1249-1273.

Shao, S.D. (2010), "Incompressible SPH flow model for wave interactions with porous media", *Coast. Eng.*, **57**(3), 304-316.

Stefanova, B., Seitz, K., Bubel, J. and Grabe J. (2012), "Water-soil interaction simulation using smoothed particle hydrodynamics", *Proceedings of the 6th International Conference on Scour and Erosion*, Paris, France, August.

Wang, Z.L., Dafalias, Y.F. and Shen, C.K. (1990), "Bounding surface hypoplasticity model for sand", *J. Eng. Mech.*, **116**(5), 983-1001.

Wang, Z.Q., Lu, Y., Hao, H. and Chong, K. (2005), "A full coupled numerical analysis approach for buried structures subjected to subsurface blast", *Comput. Struct.*, **83**(4-5), 339-356.

Yamada, S., Orense, R. and Cubrinovski, M. (2011), "Geotechnical damage due to the 2011 Christchurch, New Zealand", *Soc. Soil Mech. Geotech. Eng.*, **5**(2), 27-45.

Yang, Z. (2000), "Numerical modeling of earthquake site response including dilatation and liquefaction", Ph.D. Dissertation, Columbia University, New York, U.S.A.

Yu, S.Y., Choi, H.S., Park, K.S., Kim, Y.T. and Kim D.K. (2017), "Advanced procedure for estimation of pipeline embedment on soft clay seabed", *Struct. Eng. Mech.*, **62(**4), 381-389.

Zhang, W. and Goh A.T.C. (2016), "Evaluating seismic liquefaction potential using multivariate adaptive regression splines and logistic regression", *Geomech. Eng.*, **10(**3), 269-284.

Zhuang, H., Hu, Z., Wang, X. and Chen, G. (2015), "Seismic responses of a large underground structure in liquefied soils by FEM numerical modelling", *Bull. Earthq. Eng.*, **13**(12), 3645-3668.

CC